RSC Advances

ROYAL SOCIETY OF CHEMISTRY

www.rsc.org/advances

Preparation of Cage-like Nano-$CaCO_3$ Hollow Spheres for Enhanced CO_2 Sorption

Haoliang Ping [a], Sufang Wu [a,b*]

a. College of Chemical and Biological Engineering, Zhejiang University, Hangzhou 310027, Zhejiang, P. R. China

b. Key laboratory of Biomass Chemical Engineering of Ministry of Education, Zhejiang University, Hangzhou 310027, Zhejiang, P. R. China

*E-mail: wsf@zju.edu.cn

Abstract

Cage-like nano-$CaCO_3$ hollow spheres with different cavity diameters for CO_2 sorption were prepared using the template-directed synthesis method. Carbon sphere templates with different diameters were synthesized via a hydrothermal reaction of starch under variable conditions. Field emission scanning electron microscopy (SEM) and transmission electron microscope (TEM) images indicated that the synthesized cage-like nano-$CaCO_3$ hollow spheres had different cavity diameters of 0.52 μm, 1.62 μm and 2.93 μm. The hollow spheres shells were composed of many uniform nanoparticles with diameters of approximately 80 nm, as supported by the X-ray diffraction (XRD) results. Furthermore, the CO_2 sorption properties of the cage-like nano-$CaCO_3$ hollow spheres were analyzed by thermo-gravimetric analysis (TGA). The sorption capacity of the optimum sample with a diameter of 1.62 μm reached the

maximal theoretical value of 0.786 g_{CO2} g_{CaO}^{-1} at 600 °C and exceeded the sorption capacity of the reference nano-$CaCO_3$ sorbents by 45 %. The sorption properties of the sample within the rapid reaction stage at the different temperatures of 550 °C, 600 °C and 650 °C were also evaluated. The results demonstrated that the sample exhibited a 30 % higher sorption rate than nano-$CaCO_3$. Therefore, cage-like nano-$CaCO_3$ hollow spheres possess enhanced CO_2 sorption capacity and higher sorption rates.

Keywords: nano-$CaCO_3$, cage-like, hollow spheres, carbonaceous templates, CO_2 sorption

1. Introduction

CO_2 capture and sequestration (CCS) technologies from fossil fuel power plants are gaining interest for greenhouse gas control.[1-3] Calcium looping[4, 5] is a promising technique for CO_2 capture because Ca-based sorbents have a high stoichiometric sorption capacity, fast sorption rate and low cost of the naturally existing precursor i.e., limestone.[6, 7]

CO_2 capture by Ca-based sorbents is a reversible reaction between CaO and CO_2.[8] Carbonation of Ca-based sorbents has a theoretical stoichiometric sorption capacity of 0.786 g CO_2 per g CaO, however, few sorbents can reach or even approach this value. What's more, the carbonation rate, especially the rate of the chemical reaction-controlled stage is not sufficiently fast for the application of sorbents in industrial circulating fluidized bed technology.[9-11] The sorption properties of Ca-based sorbents, including the sorption capacity and rate, greatly depend much

on the particle size and structural morphology of the sorbents. To date, researchers in this field have endeavored to manufacture Ca-based CO_2 sorbents with a nano particle size, ranging from 10 nm~500 nm, to improve the sorption properties.[6, 8, 12-20] These approaches were inspired by the observation by Barker[19] that a 93 % CaO conversion was achieved when nanosized (~40 nm) $CaCO_3$ was used as a CaO precursor. Luo[21] found that CaO-based sorbents derived from nano-sized $CaCO_3$ provided a higher carbonation capacity and a faster carbonation rate than the CaO-based sorbent derived from micro-sized $CaCO_3$ in cyclic CO_2 capture reactions. However, studies on the preparation of CaO-based CO_2 sorbents with a nano particle size to improve the sorption capacity and rate were primarily focused on the "solid part" of the sorbents. Instead, the "void part", which has a marked effect on the transportation of CO_2 during carbonation, was ignored. Hlaing[22] synthesized the microstructured hierarchical calcite $CaCO_3$ hollow spherical sorbent composed of spike-shaped nanorods by the sol–gel hydrothermal with varying NaOH concentrations. The carbonation conversion of the synthesized sorbents was enhanced by 22% due to the hollow structure. However, the shell thickness of the synthesized sorbents, approximately 0.5 μm, still needs to be reduced. In addition, the shell is better to be cage-like porous, instead of an airtight structure, for the enhanced CO_2 diffusion.

Hollow spheres[23-25] with nanometer to micrometer dimensions represent an important class of materials and have received significant attention because of their unique structural characteristics and applications to catalysis and drug delivery. Template-directed synthesis with soft templates, such as carbon gel,[13] micelles,[26] and

gas bubbles,[27] as well as hard templates, such as polymer particles,[28] has been demonstrated as an effective approach to prepare hollow spheres. To enhance the CO_2 sorption properties of Ca-based sorbents, a hollow sphere structure has been used because of its porous structure, which can provide a large space area to ensure rapid kinetics and high sorption capacity. Broda[13] prepared Ca-based, Al_2O_3-stabilized sorbents with hollow sphere structure using carbon gel as the template, which was obtained by poly-condensation of resorcinol with formaldehyde. The sorption capacity of the sorbents reached 0.51 g CO_2 per g sorbent at 750 °C after 30 cycles. However, the preparation method was complicated, and some of the reagents used for the template synthesis were toxic. Liu[28] synthesized mesoscopic hollow spheres sorbents composed of $CaO/Ca_{12}Al_{14}O_{33}$ (approximately 6.5~13 nm) with a tunable cavity size (< 53 nm in cavity diameter) using sulfonated polystyrene (PS) as hard templates. And the CO_2 capture capacity reaches 0.58 g CO_2 per g sorbent carbonation at 650 °C for 30 min under 15 vol % CO_2. However, the cavity diameter of the hollow spheres sorbents was less than 53 nm, which impeded their direct use in circulating fluidized beds. Moreover, although the sorption capacity increased to some extent, there remains room for improvement, and the sorption rate should also be enhanced.

In this study, for possible industrial applications, micron-sized cage-like nano-$CaCO_3$ hollow spheres with different cavity diameters were fabricated using carbonaceous spheres (or carbon spheres) as templates. The structural features of the as-prepared sorbents were characterized via X-ray diffraction (XRD), transmission

electron microscope (TEM) and scanning electron microscope (SEM). The enhanced sorption properties were tested using a thermo- gravimetric analysis (TGA). In addition, the sorption performance of the as-prepared sorbents during the fast reaction stage (within 1.5 min) over a relatively low carbonation temperature range (550 °C~650 °C) was evaluated and compared with commercial nano-$CaCO_3$ sorbents.

2. Experimental

2.1 Reagents and materials

Soluble starch from potato ($(C_6H_{10}O_5)_n$, AR) for template preparation, calcium nitrate tetrahydrate ($Ca(NO_3)_2 \cdot 4H_2O$, AR), urea ($CO(NH_2)_2$, AR), and ethanol (C_2H_6O, AR) were obtained from Sinopharm Chemical Reagent Co., Ltd. Nano-$CaCO_3$ (> 95 % purity) with a particle size of 80 nm (Hu Zhou Ling Hua Ltd. China) served as the nano-CaO adsorbent precursor for reference.

2.2 Experimental section

Preparation of the carbonaceous polysaccharide sphere template. Carbonaceous polysaccharide spheres (or carbon spheres) with different sizes were fabricated via the hydrothermal reaction of starch reported in the literature.[29] Briefly, 20 g of starch was dissolved in 100 mL of deionized water under stirring. Then, the aqueous solution was transferred to a 200-mL Teflon-lined stainless steel autoclave and was maintained at a temperature range of 170~190 °C for 6 to 10 h. The puce products were washed with deionized water and ethanol several times and then dried at 60 °C for 8 h. Carbon spheres with different sizes were prepared by changing the

hydrothermal temperature and time (Table 1). Typically, a higher hydrothermal reaction temperature and a longer time resulted in the formation of larger carbonaceous polysaccharide spheres. In addition, the carbon spheres were characterized with a core-shell structure, interior solid carbonaceous core and a hydroxylation shell, which facilitated the sorption of metal cations on the templates surface.

Preparation of cage-like nano-$CaCO_3$ hollow spheres. In a typical procedure, 2 mmol (4.72 g) of $Ca(NO_3)_2 \cdot 4H_2O$ was dissolved in 100 mL of deionized water under stirring, followed by dissolution of 8 mmol (4.8 g) of urea to form a clear solution. Then, the as-prepared carbon spheres (2 g) were added and were well dispersed into the above solution, aided by sonication for 10 min. The mixture was maintained at 80 °C for 6 h with stirring to ensure the hydrolysis of urea for Ca^{2+} deposition on the surface of the carbon spheres. Subsequently, the products were washed with distilled water several times and then dried at 60 °C for 8 h before being calcined in a muffle furnace at 500 °C for 2 h under air atmosphere. A schematic representation of the formation mechanism of the cage-like nano-$CaCO_3$ hollow spheres is shown in Figure 1.

Material characterization. The morphology of the carbon spheres and sorbents was characterized by field emission scanning electron microscopy (SEM, SU8010, Hitachi, Japan). The samples were placed on a double-sided conducting resin mounted on a sample holder, and were subsequently coated for 3 min using a gold semi-high-resolution coater. For the TEM test, a dilute suspension of the samples in

ethanol was ultrasonically dispersed before it was dropped onto a copper substrate, and the solvent was rapidly evaporated. A transmission electron microscope (TEM, JEM-2100F, JEOL, Japan) with selected area electron diffraction (SAED) was used to observe the hollow sphere structure of the samples. The crystalline phases of the sorbent components were determined with X-ray diffraction (XRD, D/MAX-RA, Rigaku, Japan) using nickel-filtered Cu Kα as the radiation source. The intensity data were collected over a 2θ range of 10~80° with a step size of 0.01° using a counting time of 1 s per point.

Evaluation of CO_2 sorption. The CO_2 sorption properties were tested using thermo gravimetric analysis (TGA, Pyris1, Perkin–Elmer, America) by continuously monitoring and recording the change of sample weight during CO_2 capture. In a typical experiment, a small amount (~ 2 mg) of the sorbents were placed in a platinum nacelle, heated to 800 °C, and maintained for 10 min under high-purity nitrogen gas (N_2) as a purge at 22 mL min^{-1}, after which the temperature was decreased to the carbonation temperature. Carbonation was conducted under the mix gas with a CO_2 partial pressure of 0.02 MPa in N_2 with a total flow rate of 22 mL min^{-1} at set temperature values (550, 600, or 650 °C) for 1.5 min or 15 min. The sorption capacity and rate of the sample were calculated from the weight change and were used as indicators of CO_2 capture performance according to the following equations:

$$\text{Sorption capacity} = \frac{\text{CO2 sorption weight}}{\text{Sorbents weight}} \quad (g_{CO2}\ g_{sorbent}^{-1})$$

$$\text{Sorption rate} = \frac{\text{d (Sorption capacity)}}{\text{d t}} \quad (d(g_{CO2}\ g_{sorbent}^{-1}) / dt)$$

3. Results and discussion

3.1 Characterization of carbon sphere templates and cage-like nano-$CaCO_3$ hollow spheres

The carbon sphere templates were synthesized via hydrothermal reaction of starch, and the SEM test results are shown in Figure 2. As shown in Figure 2, the carbon spheres of different diameters, Temp-1 with 0.44 μm，Temp-2 with 1.53 μm and Temp-3 with 3.11 μm, were prepared by varying the hydrothermal treatment conditions (i.e., reaction temperature and time).

Due to the hydroxylation shell of the carbon sphere templates, Ca^{2+} was first adsorbed on the template surface before being deposited by urea hydrolysis. Therefore, cage-like hollow spheres of different diameter were obtained by completely removing the templates through calcination. Sample-1, Sample-2 and Sample-3 present the cage-like $CaCO_3$ hollow spheres, which were prepared from Temp-1, Temp-2 and Temp-3 respectively. The XRD patterns of Sample-1, Sample-2, Sample-3, and nano-$CaCO_3$ sorbents are presented in Figure 3. All of the samples show the characteristic peaks of calcite $CaCO_3$. Phases such as amorphous carbon were not detected, indicating that the carbon sphere templates were burned off by calcination. Thus, these samples only included $CaCO_3$ as the precursor of CaO for the carbonation reaction. The $CaCO_3$ particle sizes were calculated based on the Debye–Scherrer equation and are listed in Table 2.

The morphologies of the as-prepared sorbents, Sample-1, Sample-2 and Sample-3, are shown in Figure 4 (a), (b) and (c), respectively. The three samples showed an obvious cage-like hollow sphere structure, but with different cavity

diameters. The diameter of Sample-2 (approximately 1.620 μm, Table 2) was three times larger than that of Sample-1 (approximately 0.520 μm) and half that of Sample-3 (approximately 2.926 μm). Although the cavity size of $CaCO_3$ hollow spheres can be altered with the templates, the crystal particles, which compose the entire cage-like structure, remain at approximately 78 nm (Figure 4(c)) and are nearly the same as the purchased nano-$CaCO_3$ sorbents (Figure 4(d), 80 nm).

To obtain additional information about the cage-like hollow structure, the samples were characterized by transmission electron microscopy (TEM). Figure 4(e) shows a typical TEM image of the $CaCO_3$ hollow spheres. The obvious electron density difference between the dark edge and the pale center further confirmed the hollow interiors and demonstrated that the hollow sphere was composed of nano-crystal particles. The shell thickness was approximately 70-80 nm, which was within the same range of the crystallite size. These results suggested that the cage-like shells were constructed with single layers of cage-like $CaCO_3$ nano-particles, which was in agreement with the XRD results with the JCPDS 47-1743 (Table 2); consequently, they were highly porous. The corresponding selected area electron diffraction (SAED) pattern on an individual hollow sphere (Figure 4(e)) revealed that the hollow spheres were polycrystalline.

3.2 CO_2 sorption capacity of cage-like nano-$CaCO_3$ hollow spheres

The carbonation of Ca-based sorbents consists of two stages, an initial fast regime, which is controlled by chemical kinetics, and a later slower regime, which is controlled by diffusion of CO_2 in the pores or in the solid product layer**.** Figure 5

demonstrates the CO_2 uptake performance of the as-prepared cage-like nano-$CaCO_3$ hollow spheres and the commercial nano-$CaCO_3$ sorbents in the form of sorption capacity as a function of time for 15 min at 600 °C. The curves in Figure 5 show a monotonic increase of sorption capacity versus time during the carbonation period, and all of the sorbents exhibit the two typical stages. In the initial stage of each carbonation period, the sorption capacity increased sharply followed by a plateau in the second stage. Although the as-prepared samples possessed different diameters, the sorption capacity of cage-like nano-$CaCO_3$ hollow spheres surpassed the commercial nano-$CaCO_3$ sorbents and reached more than 0.63 g_{CO2} g_{CaO}^{-1}, especially in the initial fast regime. This result should be attributed to the particularly well-defined spatial structure of the cage-like nano-$CaCO_3$ hollow spheres compared with nano-$CaCO_3$ sorbents whose particles aggregated randomly; the structure of the as-prepared samples effectively exposed the CaO particles so that the inside and outside of the hollow sphere wall could easily react with CO_2 easily, which significantly improved the CO_2 sorption capacity. The sorption capacity of Sample-2, which exhibited the best performance of all the samples, reached the maximal theoretical value of 0.786 g_{CO2} g_{CaO}^{-1} in the initial 11 min at 600 °C and exceeded the sorption capacity of the reference nano-$CaCO_3$ sorbents by 45 %. In addition, the excellent sorption capacity exhibited by Sample-2 at 600 °C was markedly better than that of CaO-based hollow sphere sorbents reported by Liu[28], which was 0.58 g CO_2 per g sorbent with carbonation at 650 °C for 30 min. The reason that Sample-2, with a cavity diameter of 1.62 μm showed the best among all the samples may be that the larger sphere cavity

diameter facilitates CO_2 diffusion during the diffusion-controlled sorption stage. However, the specific surface area decreases as the sphere cavity diameter increases, which acts as a counterbalance to the enhanced CO_2 diffusion. Thus, there should be an optimum sphere cavity diameter, and in this study it is 1.62 μm. These results revealed that nano-$CaCO_3$ sorbents with different sizes of the cage-like hollow sphere structure enhanced the sorption capacity, and the optimum cavity diameter was approximately 1.62 μm.

3.3 CO_2 sorption rate of cage-like nano-$CaCO_3$ hollow spheres

Figure 6 demonstrates the sorption rate versus time of the as-prepared cage-like nano-$CaCO_3$ hollow spheres and commercial nano-$CaCO_3$ sorbents under the same carbonation conditions. Each curve presents the increasing of sorption rate with time from the beginning and reaching its peak before it decreases. As shown in the magnified part of Figure 6, the highest sorption rates of the three hollow sphere samples are approximately 0.62 $d(g_{CO2}\ g_{sorbent}^{-1}) / dt$, exceeding the reference commercial nano-$CaCO_3$ sorbents, which are considered to possess a better carbonation activity than other micro-sized or natural limestone sorbents,[17, 30, 31] by approximately 30 %. In addition, the as-prepared nano-$CaCO_3$ hollow spheres required only 11 min to achieve the maximal sorption capacity, while the sorbents prepared by Liu[28] required 30 min; thus, the cage-like nano-$CaCO_3$ hollow spheres possess enhanced CO_2 sorption rate. Interestingly, although the maximal sorption rate of the as-prepared samples appears to be the same, Sample-1 and Sample-2 reach their peaks compared with Sample-3 which has the largest cavity diameter. The reason for

this may be that an excessively large cavity diameter will hinder the heat transfer during the carbonation process and will postpone the time to reach the maximal sorption rate. In addition, Samples 1, 2 and 3 displayed a higher sorption rate than the commercial nano-$CaCO_3$ sorbents during the slow reaction stage from approximately 2.4 min after the beginning of the process, which also contributes to the enhanced CO_2 sorption capacity of cage-like nano-$CaCO_3$ hollow spheres.

3.4 Evaluation of sorption performance during the fast sorption stage at different temperatures

The carbonation temperature has a significant effect on the sorption properties. Enhanced CO_2 reaction kinetics in the fast sorption stage at a comparatively low temperature (approximately 600 °C) is favored in practical applications, especially in circulating fluidized-bed reactors (as in modern FCC units) due to the typically short contact time. The reaction activity of cage-like nano-$CaCO_3$ hollow spheres (i.e., Sample-2) in the fast sorption stage at a relatively low carbonation temperature was investigated and was compared with the commercial nano-$CaCO_3$ sorbents. Figure 7 displays the sorption performance of Sample-2 and nano-$CaCO_3$ sorbents for the first 1.5 min of carbonation performed at 550 °C, 600 °C and 650 °C. Both of the sorbents exhibit the typical sigmoid curves, for which the sorption capacity increases with carbonation temperature. The sorption capacity at 650 °C is higher than that at the other two temperatures. It can be observed that the sorption capacity of Sample-2 is always approximately 30 % higher than that of the nano-$CaCO_3$ sorbents at the same reaction temperature. When carbonation is performed at 650 °C for 1.5 min, the

sorption capacity of Sample-2 is 0.58 g_{CO2} g_{CaO}^{-1} which accounts for 73.8 % of the complete conversion of the sorbents and demonstrates a good reaction activity during the fast sorption stage.

The sorption rate of Sample-2 and nano-$CaCO_3$ sorbents at different carbonation temperatures are shown in Figure 8, and the unimodal curves reach their peaks at approximately 0.6~1 min. For Sample-2 and the nano-$CaCO_3$ sorbents, the maximal sorption rate increases with carbonation temperature. However, at the same temperature, Sample-2 exhibits a 30 % higher maximal sorption rate than the commercial nano-$CaCO_3$ sorbents. Figure 8 also shows that at the same reaction temperature, the Sample-2 sorbents exhibit a longer duration in the fast sorption stage and a higher rate during the slow sorption stage than commercial nano-$CaCO_3$ sorbents. These properties indicate an enhanced sorption performance of the cage-like nano-$CaCO_3$ hollow sphere because a later onset of the slow reaction stage means a longer carbonation time and a higher sorption capacity.

As previously mentioned, the cage-like nano-$CaCO_3$ hollow spheres show a distinct enhanced CO_2 sorption rate. There are several reasons for this phenomenon. First, the void space in the hollow structures and the cage-like morphology, as shown in Figure 3, provide much a substantial amount of room for CO_2 to diffuse during carbonation, which reduces the mass transfer resistance, hence boosting the sorption rate. Second, contrary to microporous sorbents (< 2 nm), the cage-like nano-$CaCO_3$ hollow spheres are less susceptible to pore blockage and plugging due to the volume increase from CaO to $CaCO_3$ while retaining a large surface area to ensure rapid

kinetics. Third, due to the high surface energy of nanomaterials[32], the nano-sized crystal particles that compose the entire cage-like structure also contribute to the high carbonation activity even at a relative low temperature.

4. Conclusions

In this study, cage-like nano-$CaCO_3$ hollow spheres with different cavity sizes were prepared and demonstrated enhanced sorption properties for both sorption capacity and rate. All of the as-prepared cage-like nano-$CaCO_3$ hollow spheres exhibited better carbonation activity than commercial nano-$CaCO_3$ sorbents, especially Sample-2, whose sorption capacity reached the maximal value of 0.786 $g_{CO2}\, g_{CaO}^{-1}$ in 11 min at 600 °C and exceeded the commercial nano-$CaCO_3$ sorbents by 45%. In addition, cage-like nano-$CaCO_3$ hollow spheres show a remarkable sorption rate, even over a relatively low temperature range (550 ℃~650 ℃). The enhanced sorption properties should be attributed to the special cage-like hollow sphere morphology and the small size of the crystal particles, which allowed carbonation to occur during a prolonged kinetics-controlled stage and facilitate the CO_2 diffusion during the diffusion-controlled stage. With these enhanced sorption properties, cage-like nano-$CaCO_3$ hollow spheres are promising candidates for industrial scale CO_2 capture applications in which a fast sorption rate and high sorption capacity are required.

Acknowledgements

We are grateful for finical supports from National Natural Science Foundation of

China (Grant No. 21276234).

Notes and references

1. K. M. K. Yu, I. Curcic, J. Gabriel and S. C. E. Tsang, *ChemSusChem*, 2008, **1**, 893-899.
2. J. F. M. Orr, *Energy & Environmental Science*, 2009, **2**, 449-458.
3. A. Alabdulkarem, Y. Hwang and R. Radermacher, *Applied Energy*, 2015, **147**, 258-268.
4. J. Blamey, E. J. Anthony, J. Wang and P. S. Fennell, *Progress in Energy and Combustion Science*, 2010, **36**, 260-279.
5. J. Wang, V. Manovic, Y. Wu and E. J. Anthony, *Applied Energy*, 2010, **87**, 1453-1458.
6. Z. Yang, M. Zhao, N. H. Florin and A. T. Harris, *Industrial & Engineering Chemistry Research*, 2009, **48**, 10765-10770.
7. J. M. Valverde, P. E. Sanchez-Jimenez and L. A. Perez-Maqueda, *Applied Energy*, 2015, **138**, 202-215.
8. Y. Zhu, S. Wu and X. Wang, *Chemical Engineering Journal*, 2011, **175**, 512-518.
9. M. Broda and C. R. Müller, *Fuel*, 2014, **127**, 94-100.
10. R. Digne, F. Feugnet and A. Gomez, *Oil Gas Sci. Technol. – Rev. IFP Energies nouvelles*, 2014, **69**, 1081-1089.
11. M. Broda, A. M. Kierzkowska and C. R. Müller, *Advanced Functional Materials*, 2014, **24**, 5753-5761.
12. S. F. Wu and P. Q. Lan, *Aiche Journal*, 2012, **58**, 1570-1577.
13. C. R. Müller, *Advanced Materials*, 2012, **24**, 3059-3064.
14. P. Lan and S. Wu, *Chemical Engineering & Technology*, 2014, **37**, 580-586.
15. J. Wang, L. Huang, R. Yang, Z. Zhang, J. Wu, Y. Gao, Q. Wang, D. O'Hare and Z. Zhong, *Energy & Environmental Science*, 2014, **7**, 3478-3518.
16. Y. Wang, Y. Zhu and S. Wu, *Chemical Engineering Journal*, 2013, **218**, 39-45.
17. S. F. Wu and Y. Q. Zhu, *Industrial & Engineering Chemistry Research*, 2010, **49**, 2701-2706.
18. S. F. Wu, Q. H. Li, J. N. Kim and K. B. Yi, *Industrial & Engineering Chemistry Research*, 2008, **47**, 180-184.
19. R. Barker, *Journal of Applied Chemistry and Biotechnology*, 1974, **24**, 221-227.
20. W. Liu, H. An, C. Qin, J. Yin, G. Wang, B. Feng and M. Xu, *Energy & Fuels*, 2012, **26**, 2751-2767.
21. C. Luo, Q. Shen, N. Ding, Z. Feng, Y. Zheng and C. Zheng, *Chemical Engineering & Technology*, 2012, **35**, 547-554.

22. N. N. Hlaing, S. Sreekantan, R. Othman, S.-Y. Pung, H. Hinode, W. Kurniawan, A. A. Thant, A. R. Mohamed and C. Salime, *RSC Advances*, 2015, **5**, 6051-6060.
23. X. W. Lou, L. A. Archer and Z. Yang, *Advanced Materials*, 2008, **20**, 3987-4019.
24. M.-M. Titirici, M. Antonietti and A. Thomas, *Chemistry of Materials*, 2006, **18**, 3808-3812.
25. X. Sun, J. Liu and Y. Li, *Chemistry – A European Journal*, 2006, **12**, 2039-2047.
26. B. P. Bastakoti, S. Guragain, Y. Yokoyama, S.-i. Yusa and K. Nakashima, *Langmuir*, 2010, **27**, 379-384.
27. Y. Han, M. Fuji, D. Shchukin, H. Möhwald and M. Takahashi, *Crystal Growth & Design*, 2009, **9**, 3771-3775.
28. F.-Q. Liu, W.-H. Li, B.-C. Liu and R.-X. Li, *Journal of Materials Chemistry A*, 2013, **1**, 8037-8044.
29. M. Sevilla and A. B. Fuertes, *Chemistry – A European Journal*, 2009, **15**, 4195-4203.
30. N. H. Florin and A. T. Harris, *Chemical Engineering Science*, 2009, **64**, 187-191.
31. S. Wang, S. Yan, X. Ma and J. Gong, *Energy & Environmental Science*, 2011, **4**, 3805-3819.
32. R. Valiev, *Nature*, 2002, **419**, 887-889.

Table 1. Carbonaceous templates resulting from different hydrothermal treatment conditions.

No.	T [°C]	t [h]	diameter [μm] [a]
Temp-1	180	6	0.44
Temp-2	180	8	1.53
Temp-3	190	10	3.11

[a] Mean sphere diameter size.

Table 2. Physical properties of sorbent samples prepared with different templates.

No.	Particle size [nm] [a]	hollow spheres diameter [μm] [a]
Sample-1	78	0.52
Sample-2	76	1.62
Sample-3	72	2.93
nano-$CaCO_3$	80	—

[a] Mean sphere diameter size.

Figures and Captions:

Figure 1. Diagram of the formation mechanism of cage-like nano-$CaCO_3$ hollow spheres.

Figure 2. Scanning electron microscopy (SEM) images of the carbon sphere templates prepared under various conditions: (a) for Temp-1; (b) for Temp-2 and (c) for Temp-3.

Figure 3. XRD patterns of the Sample-1, Sample-2, Sample-3 and nano-$CaCO_3$ sorbents.

Figure 4. SEM images of the (a) Sample-1, (b) Sample-2, (c) Sample-3, (d) commercial nano-$CaCO_3$ sorbents and a (e) TEM image of Sample-2 with the SAED pattern.

Figure 5. Sorption capacity during carbonation of sorbent samples.

Figure 6. Sorption rate during the carbonation of sorbent samples.

Figure 7. Sorption capacity during the carbonation of sorbent samples.

Figure 8. Sorption rate during carbonation of sorbent samples.

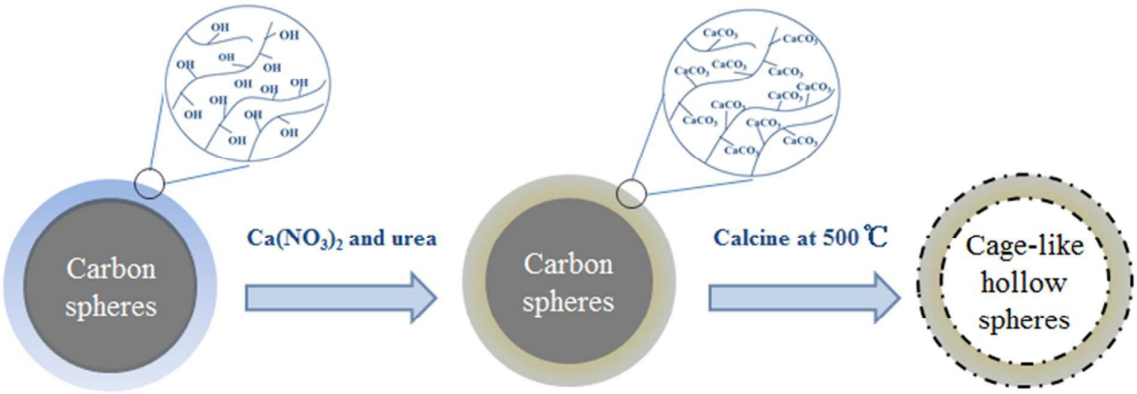

Fig. 1

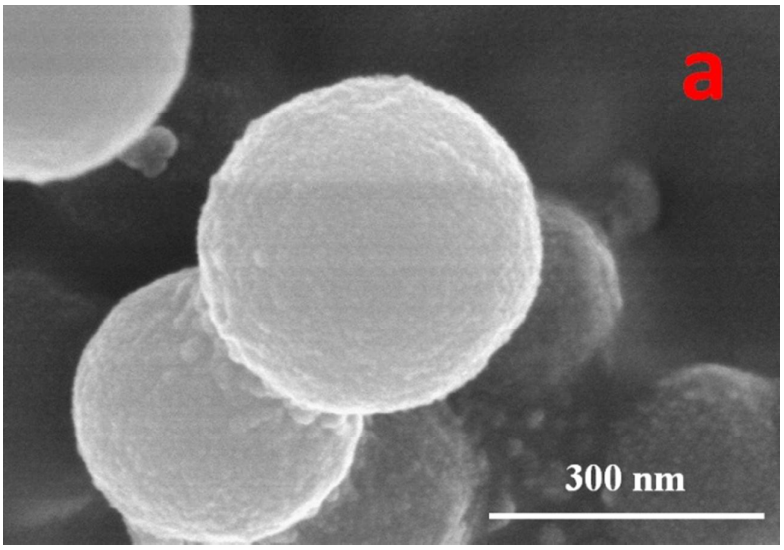

Fig. 2 (a)

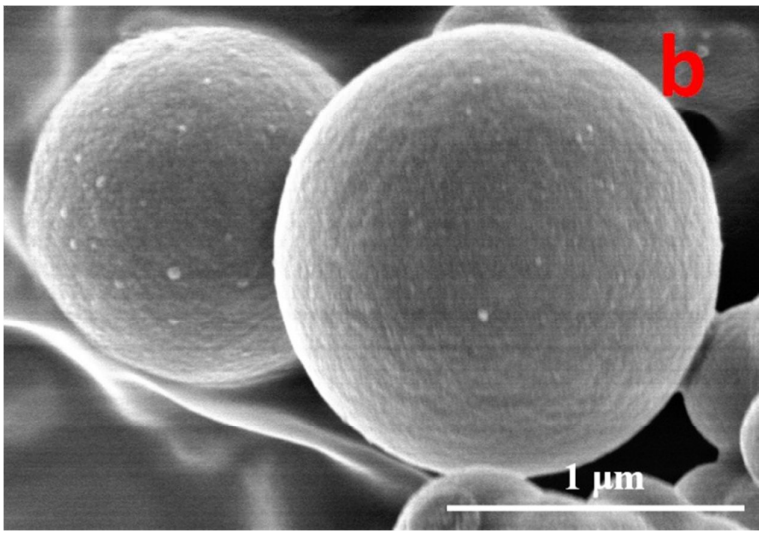

Fig. 2 (b)

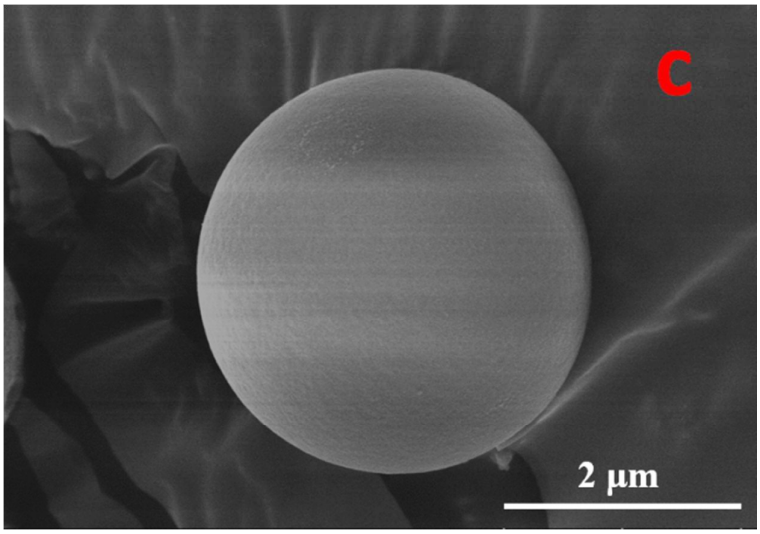

Fig. 2 (c)

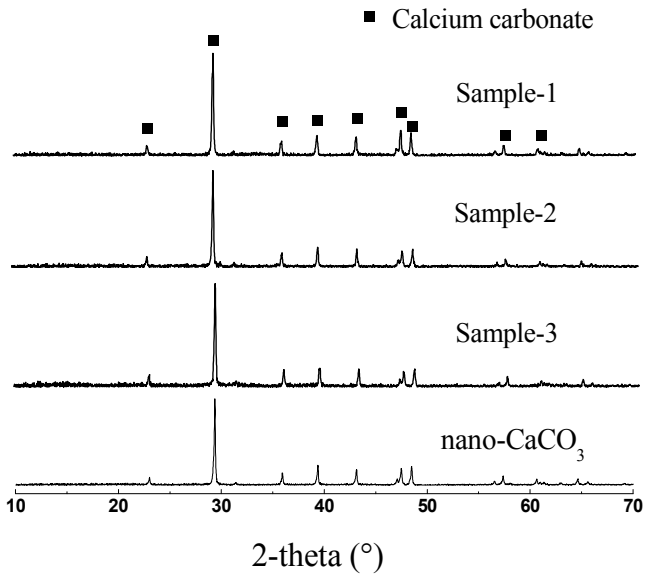

Fig. 3

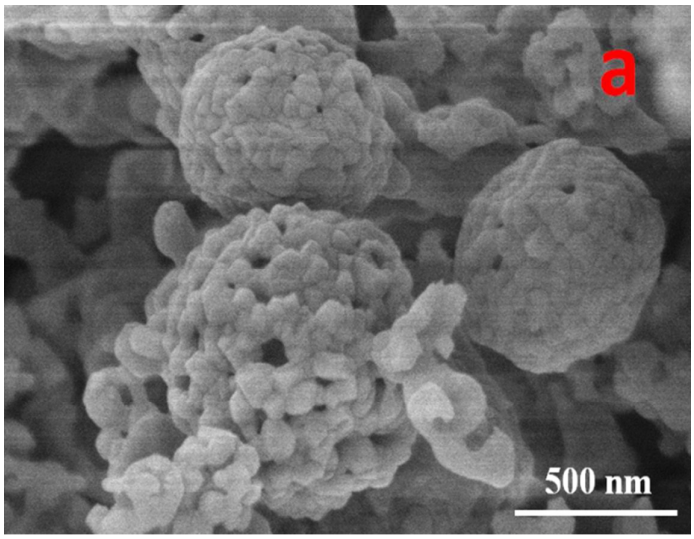

Fig. 4 (a)

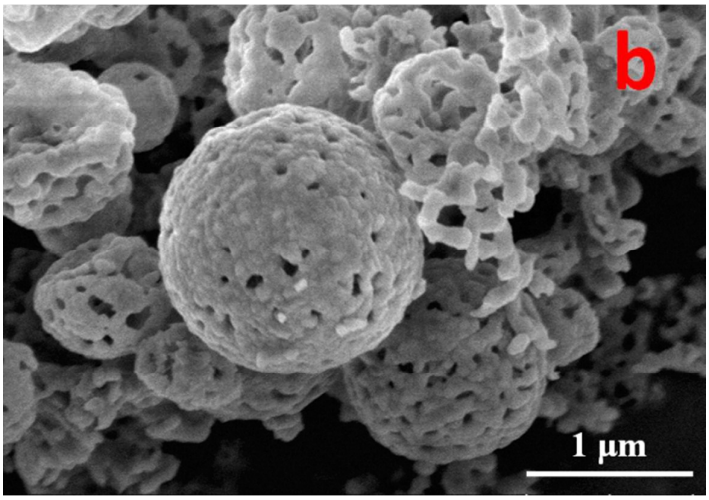

Fig. 4 (b)

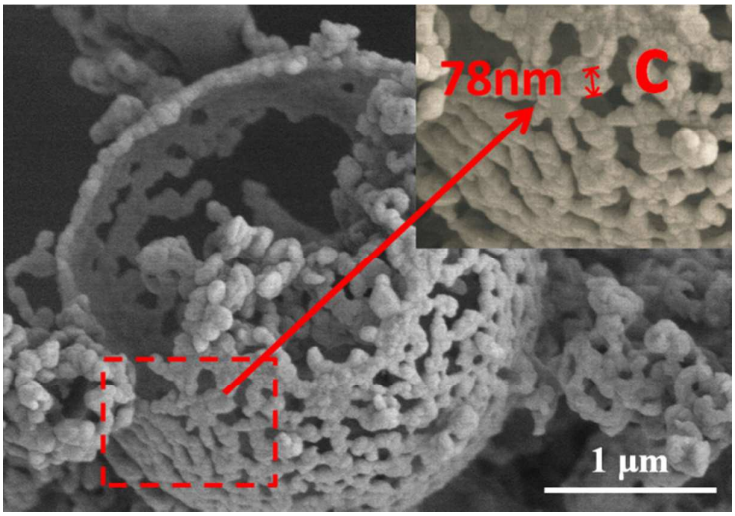

Fig. 4 (c)

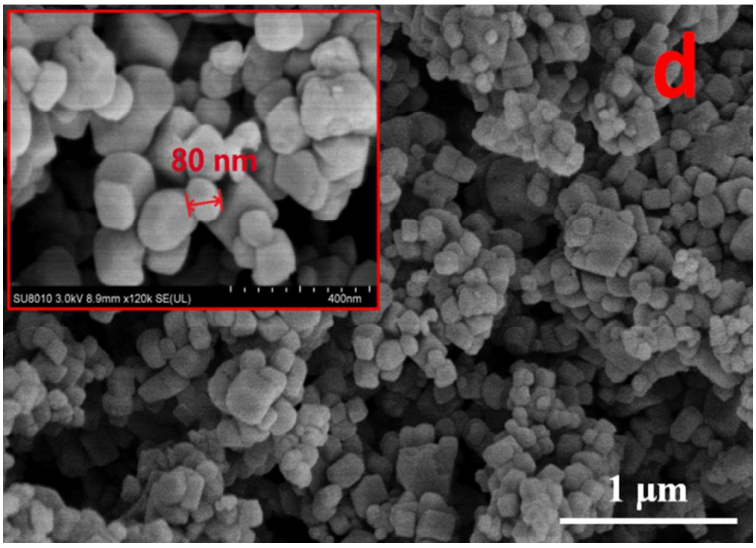

Fig. 4 (d)

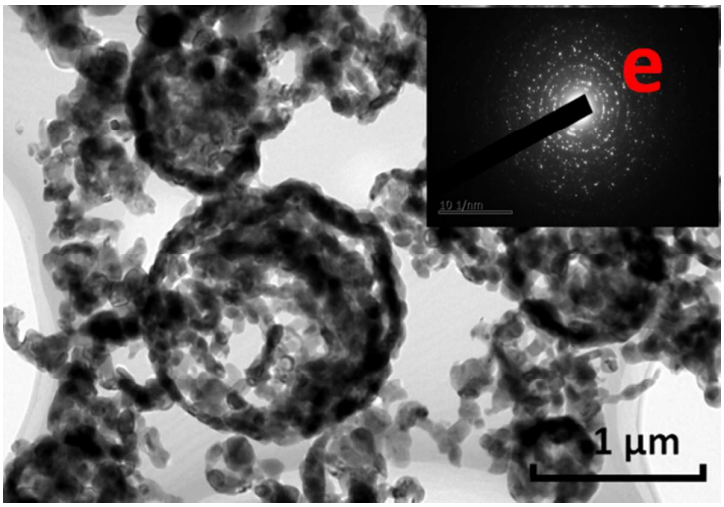

Fig. 4 (e)

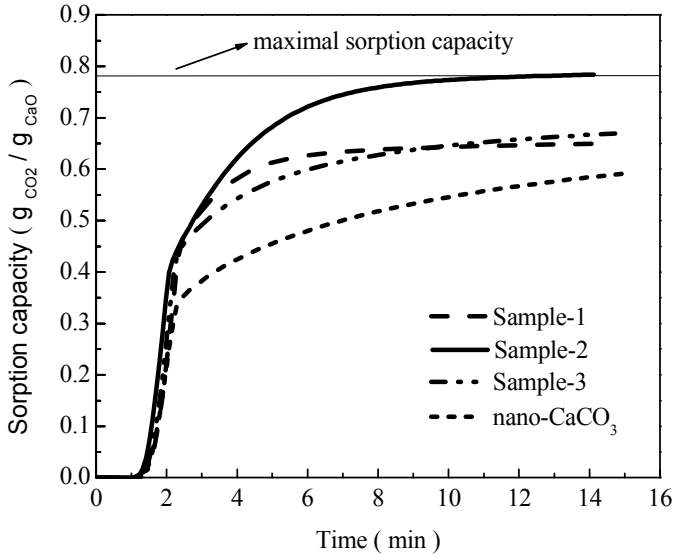

Fig. 5

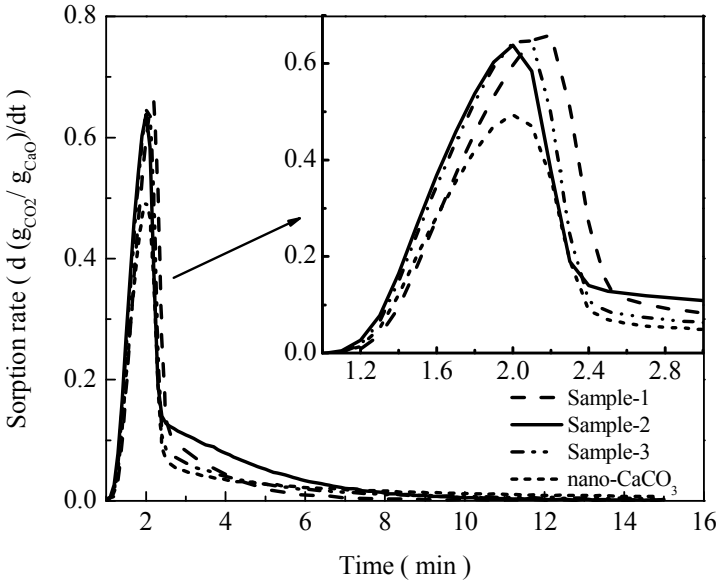

Fig. 6

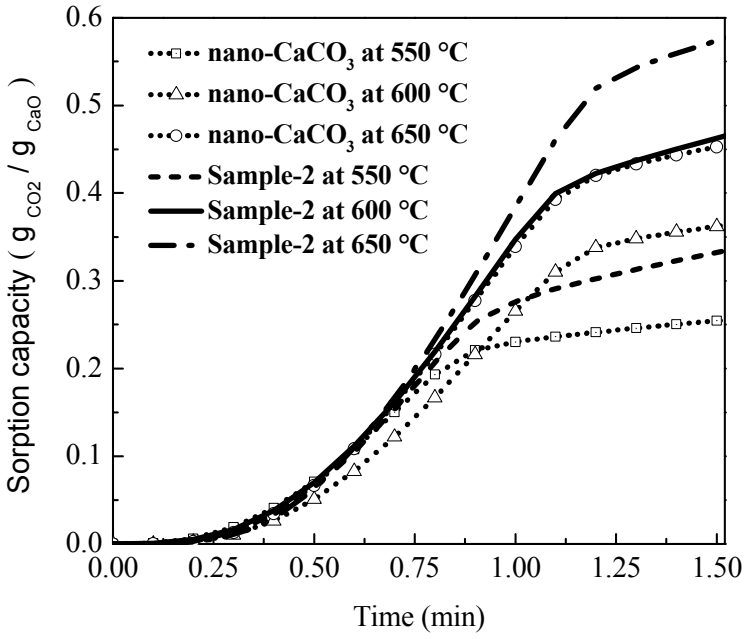

Fig. 7

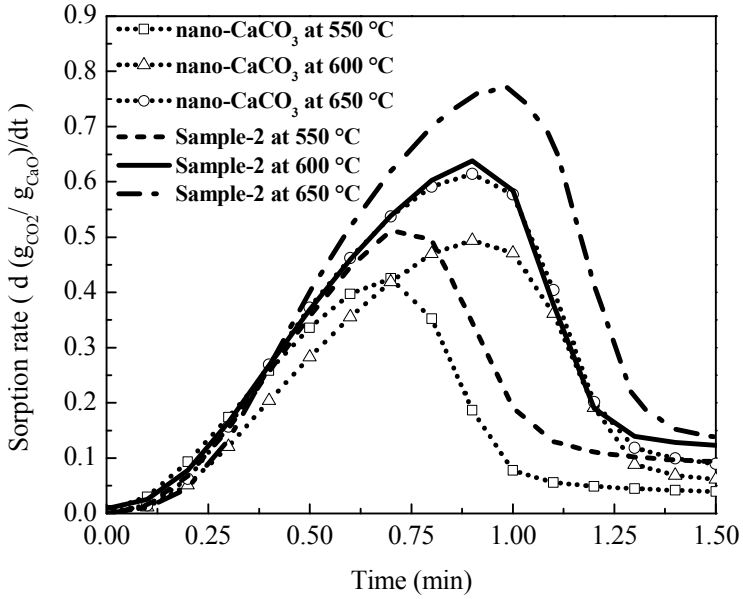

Fig. 8